Chapter 4

Energy Storage Using Hydrogen Produced From Excess Renewable Electricity: Power to Hydrogen

Marcelo Carmo[1], Detlef Stolten[1,2]
[1]*Forschungszentrum Jülich GmbH, Jülich, Germany;* [2]*RWTH Aachen University, Aachen, Germany*

MOTIVATION

In recent decades the threat of climate change, the potential of renewable energy in terms of capacity as well as cost reduction, has been significantly underestimated. Besides the COP 21 agreement that focuses on the reduction of CO_2 emissions as a major driver for developed countries, there is a second equally important driver emerging from developing countries in the form of the reduction of local emissions. The CO_2 issue, while certainly serious, is typically perceived by the layman as being somewhat remote, whereas the issue of local emissions is a great deal more tangible. In real terms the latter is therefore more pressing, and as such it requires long-term political focus. Nonetheless, the prospect of rising sea levels has given impetus to the drive to reduce CO_2 emissions, in both developed and developing nations. This is, of course, more difficult to address in developing countries because of more stringent cost constraints on mitigating efforts. The use of renewable energy serves to bring down expenditure on fuel imports, potentially also on infrastructure such as electric grids and comprehensive gas grids for developing countries. There is therefore a necessity and an opportunity for worldwide efforts to combat climate change in all nations, regardless of the economic status.

This purpose of this chapter is to elucidate the opportunities, requirements, and constraints involved in the use of renewable sources for energy storage. It will focus on chemical storage, which is suitable for *long-term* storage. Short-term storage options will be briefly outlined, including power to heat options.

Science and Engineering of Hydrogen-Based Energy Technologies. https://doi.org/10.1016/B978-0-12-814251-6.00004-6

Long-term strategies are subject only to relatively minor losses during storage—such as self-discharge or gas slip—and very low specific investment cost for the storage units because the turnover frequency of the storage capacity is low, increasing the specific cost of the energy stored.

RENEWABLE ENERGY, VOLATILITY, AND STORAGE

The paradigm of the existing power supply chain is load-following of the demanded power production. In a fully or mostly renewable power production setup, the power input is determined by the weather situation. Hence, temporal over- and underproduction are inherent, changing the paradigm completely into harnessing most of the renewable energy attainable, regardless of the actual demand at the time.

Realizing that the electrical grid provides no storage capability—other than a gas grid does—the electrical energy harnessed needs to be used instantaneously at some point of the grid. Relevant options are setting up a strong transportation grid to equilibrate renewable energy input of different nature—e.g., wind versus solar—or different climate zones. The latter generally require transportation over very long distances like in the thousand kilometer range. The other set of options is storage of the power overproduced.

If that route is pursued, underproduction can be covered either by using fossil fuels such as natural gas or by reconverting the stored energy back again to electricity. Natural gas provides great flexibility options particularly when transforming the power production to renewables. The energy from temporal overproduction can then be fed back to other energy sectors such as transportation, households, or industry. The scheme is more often referred to today as sector coupling. Beyond improving the actual energy balance, it provides the opportunity to interconnecting the power sector already at an early stage of transformation with the other energy sectors.

Grid Stabilization and Short-Term Storage

Currently, grids get stabilized by a rotating momentum created by the rotational energy of the turbines and the generators. In case of increasing power demand, the rotating frequency decreases, which is mirrored in the generated frequency for the grid and serves as a signal to increase the power input by gearing up the power plant until the desired standard frequency is reached. The property of rotating masses exhibiting inertia is equivalent to describing them in the amount of stored energy. For this reason the existing grades are pretty resilient to very fast load changes and need to be supported by additional input only in the range of a few minutes and not instantaneously. This is handled today, for example, by swiftly adjusting steam power plants that can store energy in the steam vessels or by pumped hydropower plants. Thereafter, further power sources can be activated in the range of approximately 15 min.

The scheme is expected to change dramatically if no rotating masses are grid-connected anymore. Experience with a long-distance DC–DC transport line in China toward Hong Kong indicates that without rotating masses—or in this case, negligible rotating masses, which would also be the case in renewable scenarios—the response time needs to be in a 10 to 100 millisecond range rather than in the minute range. This is important to note for the development of electrolyzers that might help stabilize the electric grid alongside battery units or other devices such as fly wheels. Whereas batteries can instantaneously respond to load changes they are limited in sustaining the response over a longer time owing to the limited capacity, the use of electrolyzers for grid stabilization is still to be proven. Batteries, if not fully charged, can operate in either direction to compensate a positive residual load, i.e., less energy provided in the grid than demanded, or a negative residual load, i.e., less demand that the amount of energy produced at that moment in time. Electrolyzers can basically deliver the same service when being operated below the full capacity. When operated at full capacity, electrolyzers can only shed off load and compensate that way for positive residual load. These dynamic processes need further investigation on the grid side and particularly for electrolyzer systems.

Energy Security and Long-Term Storage

Whereas the short-term, i.e., hourly and daily, fluctuation of renewable energy is very obvious and palpable. It is less intensely discussed that renewable energy also has strong longer-termed fluctuations, leading to seasonal over- or underproduction of power as well as to zero or close to zero production for sustained periods, such as multiple days or even multiple weeks. Just to elucidate the order of magnitude of required storage for backing up a 2-month period of no power input, one can take one-sixth of the annual power consumption of a country. This would, for instance, for Germany result into a storage requirement of about 80 TWh. Assuming that 50% of the regular power requirement can be covered by other measures such as power transportation from other regions or smart reduction of the power consumption for the time, it would still amount 40 TWh. Different assumptions for storage requirement in the long run for Germany differ from 30 to 60 TWh. This does not yet include the requirements of transportation and industry. Comparing these values with the existing capacity of pumped hydro storage of 0.04 TWh, there are obviously three orders of magnitude between the requirement and the existing storage capabilities of pumped hydro, disqualifying this technology for long-term storage of energy notwithstanding its paramount role for grid stabilization. When looking at hydrogen storage, the two questions arising from these considerations are whether the chemical storage of hydrogen delivers higher storage densities than mechanical storage does and whether there are viable concepts of storing large quantities of hydrogen. A brief example

might show the enormous energy density of gas storage. Hydrogen contains 3 kWh per standard cubic meter and gets compressed for mass storage to at least 100 bars, leading to an energy content of 337 kWh per cubic meter stored and real gas behavior considered. For pumped hydro storage in comparison, the potential energy of an elevated basin can be harnessed. This leads to about 0.8 kWh for 1 m^3 stored and a difference in altitude of the two water basins of 300 m assumed. Hence, the gas storage provides about 400 times the energy per unit volume, nearly delivering the three orders of magnitude required. The second question to be answered is whether there are appropriate means of storage for hydrogen in very large quantities.

The basic storage options for large quantities of hydrogen are underground storage of gaseous hydrogen, liquid hydrogen storage in large containers, or chemical storage of hydrogen, such as in liquid organic hydrogen carriers (LOHCs) or as chemical components such as methanol or Dimethyl ether (DME). This order also reflects the efficiency of the storage pathways. For liquid hydrogen storage, it is to be considered that active cooling to the level of liquefaction is most efficient at very large installations. Hence, in all downstream steps in shipping and storing up to the point of usage, cooling is performed passively by using the evaporation heat originating from hydrogen boil off. In this case the efficiency is dependent on whether the hydrogen can be effectively used elsewhere in the system or needs to be discarded, i.e., burnt. A similar argument is valid for the liquid hydrogen organic carriers that need heat to release the hydrogen. The heat amounts to about one-third of the energy of the hydrogen stored. If this heat is available from other sources, such as off-heat in industrial processes or geothermal energy, it might not harm the energy efficiency much. As for the chemical components such as methanol, the energy pathway includes the production of the chemical component, yet also the hydrogen production and storage as well as the provision of the carbon reaction partner from biomass or CO_2 is to be considered.

Finally, the choice of a storage option also depends on the end use of the hydrogen. Table 4.1 shows a collection of typical data for road transportation.

First of all it is important to note that hydrogen production via electrolysis is listed in Table 4.1 with an efficiency of 70% [1–3]. This is due to the fact that the lower heating value of hydrogen is considered because, in transportation applications, polymer electrolyte membrane fuel cell (PEMFC) condensation of the water produced is not feasible. When comparing hydrogen applications in the stationary sector with condensing boilers, the higher heating value (HHV) can be taken. Hence, 70% efficiency considering the lower heating value and 80% considering the HHV can be achieved with the same electrolyzer. The storage and distribution chain of gaseous hydrogen can be assumed to be at an efficiency of 90%, encompassing transportation to a storage site, compression to storage pressure of about 100–200 bar, and transportation to its end-use site. The value of 90% is a good value for any first estimation, yet it might vary strongly depending on the specific conditions [4].

TABLE 4.1 Impact of Different Storage and End-Use Options on the Total Efficiency

Applications	Electrolysis (%)	Methanation/ Fuel Production (%)	Storage Distribution (%)	Fuel Cell/ Electric Drive Train (%)	Internal Combustion Engine + Drive Train (%)	Total Efficiency (%)
1. GH_2 + FC Passenger car	70	–	90	60	–	38
2. GH_2 + FC Truck	70	–	90	50–60	–	32–38
3. GH_2 + ICE Passenger car	70	–	90	–	25	16
4. GH_2 + ICE Truck	70	–	90	–	40	25
5. GH_2 + methanation + ICE	70	80	90	–	25	13
6. GH_2 + methanation + ICE Truck	70	80	90	–	40	20
7. LH_2 + FC Passenger car	70	–	63	60	–	26
8. Liquid biofuel		50	95		25	12
9. Liquid CO_2-based fuel	70	55–80			25	10–14
10. Gasoline		90	90		25	20
11. Battery electric cars	–	–	80	85		68

For cars and trucks, efficiencies can be estimated using standard driving cycles, such as the NEDC for Europe, JCO8 for Japan, US06 for the United States, and the most recent Worldwide Harmonized Light Duty Vehicles Test Procedure (WLTP) [5]. All of them have in common that they test the vehicles under different conditions of speed and acceleration trying to represent the average use of vehicles in cities and on county roads and highways. There are notable differences in individual use to be expected, yet these standards are the best measures for comparison available. As older standards were soft on acceleration and top speed, the WLTP is more realistic.

Average efficiencies over a driving cycle for the different propulsion technologies are given in Table 4.1 as 60% for the fuel cell drive train, 25% for the drive train of internal combustion engines for vehicles, and 40% for long-haul trucks owing to the fact that these have more efficient diesel engines and that highway driving predominates. The values given here are estimates based on literature sources that typically provide data on efficiencies for specified points of operation or fuel economy values [6–9]. In the power-to-fuel route, hydrogen and CO_2 are used to produce synthetic fuels. Starting from hydrogen, methanation can achieve efficiencies of approximately 80%, while liquid fuel synthesis varies between 55% and 80% depending on the process route and the selected fuel [10,11]. An optimized Fischer–Tropsch process with exceptional recycling loops can achieve a plant efficiency of approximately 80% and a total efficiency of 14%. Fischer–Tropsch biofuels produced via gasification of biomass reach similar well-to-tank efficiencies of approximately 50%. Extraordinarily efficient is the use of electricity in a battery electric drive train with 68% in total, resulting from 80% storage and distribution efficiency and 85% efficiency of the drive train [12].

Hence, the battery electric drive train is the benchmark for what is achievable with fuel based on electricity, the so-called electrofuels. Efficiency considerations are sometimes criticized as of secondary order, yet with renewable energy efficiency stands as a proxy for cost and spatial requirements for the installations because renewable energy is to be harnessed at a very low energy density of the respective energy source such as wind or sun. The low energy density translates into relatively high energy cost through the capital expenditure (CAPEX) and into relatively large areas needed for the installations to harness the energy, such as photovoltaic (PV) fields or wind farms. This leads to the requirement of higher efficiency in other parts of the energy pathway to keep the total cost at bay.

Hydrogen Applications

This paragraph discusses the implications of the different options using renewable hydrogen. The most efficient use of hydrogen in transportation is as gaseous hydrogen for vehicles with a fuel cell (#1, Table 4.1), resulting in an efficiency of 38%. This compares with 20% efficiency in vehicles with internal

combustion engines today based on gasoline, representing the lower benchmark. When using an internal combustion engine, the efficiency would drop to 16%, owing to the lower top efficiency and particularly to the lower part load efficiency (#3, Table 4.1). Because natural gas combustion engines already exist and the storage of natural gas aboard a vehicle is somewhat easier than that of hydrogen, methanation of the hydrogen to use synthetic natural gas (SNG) could be an option. With an efficiency of methanation of 80%, the efficiency of the whole energy pathway would drop to 13% and the cost would rise accordingly, provided the CO_2 for the synthesis is taken for granted or even more if it is to be paid for.

This comparison shows that it is sensible to stick with the simplest fuel, which is hydrogen, and electrochemical conversion via a fuel cell instead of an internal combustion engine, as long as these technologies apply for the use case. Fuel cell vehicles are being constantly introduced into the market by Hyundai and Toyota these days and are being developed by many other car manufacturers. The situation is different for trucks, however. To clarify the difference, long-haul trucks are being compared with the statement for passenger vehicles.

Long-haul trucks run on a much higher efficiency of the diesel engine of about 40%, need about 200−300 kW of power and a lifetime expectancy of more than 20,000 h compared with 5000 h for passenger cars. Long-haul trucks also run on high power for most of the part of their operation. Bearing in mind the characteristics of internal combustion engines, which provide an efficiency of 47% in the most efficient point of operation [6] and fuel cells and exhibit particularly benign part-load characteristics and a decreasing efficiency with increasing load [9], the advantage of efficiency of fuel cells diminishes for this application. That can be compensated by choosing a larger fuel cell, which in turn leads to higher investment, making hydrogen combustion engine an alternative to be considered. The latter would produce no soot as fossil fuel motors do, yet it would need NO_x clean-up. Another alternative would be the route via methanation using CH_4 as a fuel with a combustion engine. For trucks these options would compare efficiency-wise to 32%−38% for gaseous H_2 with a fuel cell [#2, Table 4.1], with a combustion engine to 25% and for SNG with a combustion engine to 20%. Combining the use of SNG with a fuel cell is likely to be referred to niche markets because the reforming process with an efficiency of 80% would further reduce the total efficiency to 16%. This shows that for long-haul trucks the picture is not yet clear, further development and demonstration is needed, and barriers that have been overcome already for passenger cars are still an issue for the much higher requirements.

Whereas hybridization is not so effective at a constant high power demand because the limited battery capacity is quickly drained, it comes in strongly in city traffic, enabling regenerative braking and powerful acceleration with relatively small engines, be it fuel cell engines or motors. For this reason, fuel

cell buses are viable for public transport. As for the efficiency comparison in this use case, fuel cells are ahead of internal combustion engines such as in passenger cars; however, combustion engines can also be hybridized. Buses and delivery trucks are much closer to passenger vehicles, and indeed most of the urban fuel cell buses are equipped with derivatives of fuel cell systems from passenger cars, sometimes using the same hardware. Coaches on the other hand are similar in their characteristics to long-haul trucks.

Liquid hydrogen can be considered an alternative over gaseous hydrogen for its high energy density in the use case of a passenger car. Liquefaction consumes about one-third of the energy content of the hydrogen energy, leading to a total efficiency of 26% for the passenger car with a fuel cell compared with 38% when fueled with gaseous hydrogen. For sake of easy use for the consumer, the fuel would be gasified and compressed for storage in a car anyway to get around the issue of the necessary hydrogen evaporation for cooling a liquid tank, which leads to fuel consumption when the car is not used for a longer time and bars access to public parking garages. The picture of efficiency changes, if imported hydrogen is considered. Aboard naval vessels, hydrogen will not be transported as compressed gas, but in the liquid stage or by liquid organic hydrogen carriers or as chemical substances like methanol. Taking the case of liquid hydrogen delivered to a port, the efficiency argument held against liquefaction above is no longer valid because the step had to be taken for overseas transport anyway and advantage of the easier distribution of liquid hydrogen can be exploited. Yet, what about cost and specific land use at the site of production owing to the less efficient step? That can be compensated for by choosing preferable sites for harnessing renewable energy.

As a case in point, wind energy can be harnessed in Patagonia at 5000 to 5500 full load hours, whereas in the North Sea about 4000 full load hours are available, making it nearly up for liquefaction in the case of hydrogen production in Patagonia; where the specific land use is a lot higher compared with the hydrogen production in the North Sea. Compared with 2000 full load hours of wind power production at many sites in the world, liquefaction for transportation poses no barrier, neither in terms of efficiency nor cost.

The last area for application here is what is called the power-to-fuel route, making a liquid fuel out of electricity by hydrogenating biomass or using CO_2 as a carbon source. The efficiency of these liquid fuels drops down to 12% and 9%, respectively. Yet, this is not a reason to rule out these fuels. Whereas they will hardly be competitive where easier alternatives exist, like the option [#1, Table 4.1] for passenger cars, CO_2-lean liquid fuels will be needed in aviation and some special applications. For the time being, a fuel switch in aviation is inconceivable until 2050 and not even likely in the decades thereafter, as aviation relies even more on the high energy density of liquid fuels than any other sector of transportation.

This discourse took just one property to elucidate options for transportation trying to depict the potential of hydrogen and the vectors for its application.

Designed to structure decision-making on the one hand, it revealed the complexity involved. What can be taken from this exercise is mainly the following:

- The complete energy pathway is to be considered; otherwise the results will very likely be wrong.
- Whether an energy pathway makes sense or not, strongly depends on the use case.
- For the sake of efficiency—as a proxy of cost and specific land use—the simplest fuel pathway is the best. The use case defines whether it can be applied or not.
  - Direct power use provides efficiencies around 90%–95%.
  - Power with battery storage provides efficiencies around 85%.
  - Fuel cells with hydrogen achieve efficiencies of 38%.
  - Hydrogen with methanation in a passenger car achieves of an efficiency of 13%.
- Use cases similar at the first glance can be very different, such as passenger cars and long-haul trucks, either ones being road transportation vehicles.
- Use cases looking dissimilar, such as passenger cars and urban buses, can be pretty similar.
- Hydrogen is the basis for synthetic fuels.
- Synthetic fuels attain only about half of the energy pathway efficiency of today's energy pathways.
- Nonetheless, synthetic fuel needs to be considered for specific applications such as aviation.

When assessing these fuel choices, many more properties need to be considered, yet this simple approach already provides some structure to the issue, shows the complexity, and provides insight how valuable hydrogen is for the future fuel infrastructure, be it as elementary hydrogen, syngas, or liquid fuel. The primary renewable energy source for hydrogen worldwide will be renewable power, and the primary technology the hydrogen will be produced of power is electrolysis [13]. Thus, the technological specifics of electrolysis will be outlined in the second part of this chapter.

Water Electrolysis—A "Game Change" Technology

For long-term storage, hydrogen is an essential building block along the energy pathway. It can be generated from electricity via electrochemical water splitting, i.e., water electrolysis, or by applying thermochemical cycles. Whereas water electrolysis is a well-established process, thermochemical water splitting is still under development. Thermochemical water splitting works well together with concentrated solar power installations, which provide the required high temperature. Because neither concentrated solar power installations nor the thermochemical processes are established technologies,

this route will not be further discussed in detail, yet it should be kept in mind for further development.

Although water electrolysis is a very well-established technology for producing high-grade hydrogen in the chemical and process industries, the worldwide share of hydrogen produced by electrolysis is only about 4%, whereas steam methane reforming covers about 96%. Steam methane reforming is cheaper owing to the fact that natural gas is cheaper compared with electrical power and that electrolyzers are not yet being mass-produced and optimized for low cost application, which is crucial for the generation of hydrogen as an energy carrier. Hence, the second part of this chapter will focus on electrolysis technology with regard to cost savings through design, material choices, and operating conditions.

HYDROGEN GENERATION VIA ELECTROLYSIS

Brief History of Water Electrolysis

Technologies to split water into hydrogen and oxygen using electricity have been present in our industry realm for more than 100 years. However, unfortunately, clean hydrogen produced by water electrolyzers in the 21st century is still very marginal compared with full hydrogen demand worldwide. The main reason is that splitting water to hydrogen with any sort of available electricity is from a cost point of view still less favorable than catalytically reforming methane or natural gas into hydrogen. To date, hydrogen is primarily produced by steam reforming of natural gas, via partial oxidation of mineral oil or coal gasification. To some extent, there is, however, nowadays an important market for the onsite generation of hydrogen using electrolyzers, pure hydrogen that is typically needed in the glass, steel, food industry, power plants for generator cooling and in the manufacture of electronic components, life support for military applications, and other small niches.

Clearly, the balance between electrolytic hydrogen and hydrocarbon-derived hydrogen (catalytic reformed) depends very much on the relative costs of the fossil-based hydrocarbon (typically very unstable) and electricity (partially stable when supplied, for instance, by a hydropower plant in a country with reliable energy infrastructure). After all, advantages for producing electrolytic hydrogen include the simplicity of production, the lack of pollution, easy scalability, and the availability of raw materials necessary for the electrochemical reaction to take place. After many decades of its demonstration and industrial usage, state-of-the-art technologies of water electrolysis are still alkaline (using a liquid alkaline caustic electrolyte), and acidic electrolysis (where a polymeric electrolyte membrane [PEM] electrolysis) is used. In addition, a strong market niche also exists using electrolysis to produce chlorine for the chemical industry, the so called chlor-alkali electrolysis, a technology, however, that is not the scope of this chapter.

Alkaline Water Electrolysis

The principles of alkaline water electrolysis were introduced more than 100 years ago, and many electrolysis plants have been constructed and reliably operated to date. By the end of the last century, a few electrolyzer facilities were still in operation, such as the one in Rjukan in Norway exceeding 60,000 Nm^3/h and in Aswan Egypt with a capacity of up to 30,000 Nm^3/h. More facilities shall still be operational in Reykjavik Iceland, in Cuzco Peru, and in other countries around the globe. These plants were usually dedicated to generate hydrogen to be subsequently used for ammonia synthesis and finally for the fertilizer production, always when and where cheap electricity from a hydropower plant was locally available. Large-scale electrolyzer facilities have mainly used low-pressure electrolyzers, with the capacity of these electrolyzers ranging around 200 Nm^3/h of hydrogen. The Lurgi pressurized electrolyzer shown in Fig. 4.1A produced hydrogen at 740 Nm^3/h, which corresponds to an electrical output of approximately 3.6 MW. The stack was assembled with 560 cells having an active area diameter of 1.60 m and, depending on the number of cells, the stack length could achieve 10 m. In contrast to the Lurgi electrolyzer, the Bamag electrolyzer operated at atmospheric pressure (Fig. 4.1B) using rectangular electrodes with an active area of approximately 3 m^2 and usually with 100 cells with a production capacity of approximately 330 Nm^3/h of hydrogen.

In the 1980s and 1990s, large research projects were running as a natural response to the second oil crisis including a variety of R&D projects within Jülich and DLR; a 10-kW Electrolyzer DLR HYSOLAR with 500 cm^2, a 10-kW Electrolyzer FZJ 3 bar with 1000 cm^2, a 26-kW Electrolyzer PHOEBUS 7 bar with 2500 cm^2, and 5-kW Electrolyzer PHOEBUS 120 bar with 500 cm^2 active area. These research projects had the main goal to demonstrate innovative approaches to increase the power density and operating pressure of alkaline electrolysis. Fig. 4.2 shows pictures of these projects, demonstrating the complexity of these systems and the R&D trend toward larger electrode active

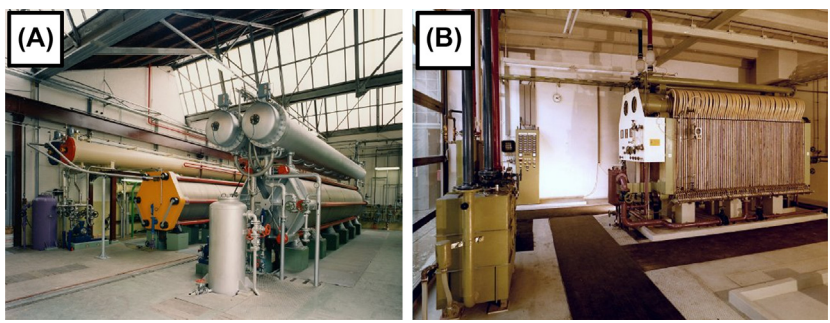

FIGURE 4.1 Lurgi pressurized electrolyzer (A) 740 Nm^3/h of hydrogen and a Bamag atmospheric electrolyzer (B) with a capacity of 300 Nm^3/h of hydrogen.

areas and higher operating pressure. In addition, it was also the aim to increase the current density, lower the cell voltages, and increase operating temperatures to reduce capital and operational costs of alkaline water electrolyzers.

Alternatively, an incremental modification of the cell configuration to minimize the ohmic drop and the development of novel electrodes to reduce the sum of the anodic and cathodic overpotentials were consistently pursued. In cooperation with the center in Jülich, Lurgi demonstrated that, by using Raney Ni electrodes and NiO diaphragms (Fig. 4.3), it was possible to reduce the single cell voltage from 1.92 to 1.6 V at a constant current density of 0.2 A/cm^2 or to 1.72 V at 0.4 A/cm^2, where the gain was obtained by means

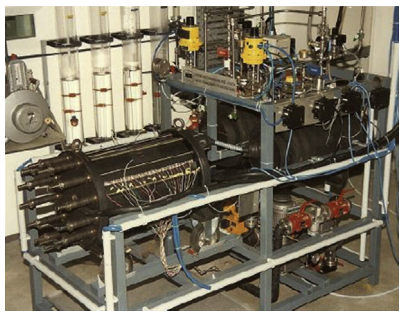

10 kW Electrolyzer DLR HYSOLAR 500cm²

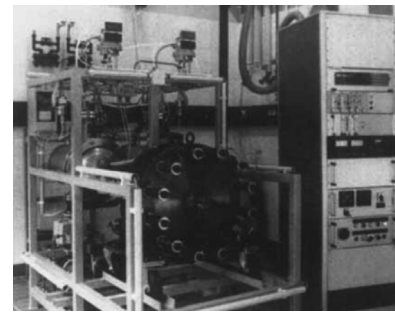

10 kW Electrolyzer FZJ 3 bar 1.000 cm²

26 kW Electrolyzer PHOEBUS 7 bar with 2.500 cm²

5 kW Electrolyzer PHOEBUS 120 bar with 500 cm²

FIGURE 4.2 Electrolysis activities in Jülich (electrodes, diaphragm, stack, and system development) from 1979 until 2002.

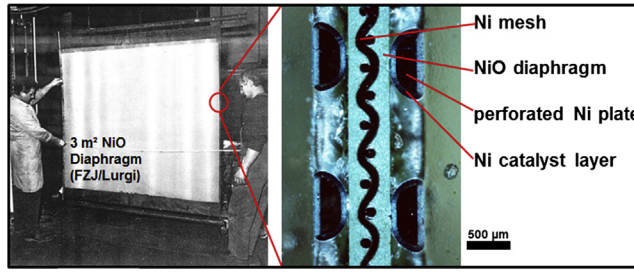

FIGURE 4.3 Research and Development in Jülich of an NiO diaphragm for alkaline water electrolyzers.

of a zero-gap cell configuration (minimal distance between electrodes and diaphragm). As part of a government-funded project, this technology led to the construction of a 32 bar pressurized electrolyzer with an output of 1 MW.

In other German national projects (HySolar [14], SWB [15], PHOEBUS [16]), different alkaline water electrolyzers were developed, constructed, and tested. Nowadays, according to NEL, the cost of large-scale alkaline electrolyzers will be less than 700 $/kW by 2020[1]. Today, alkaline electrolyzers are supplied commercially by a few companies, and a not extensive overview of leading manufacturers is shown in Table 4.2. Most manufacturers currently specify a limited lower partial load range for the alkaline electrolyzers. The lower partial load range seems to be detrimental when coupling in particular to renewable energy sources where a nonnegligible fraction of the capacity for electrolysis cannot be used for hydrogen production. In addition, current alkaline electrolyzers are limited to still reasonably low current densities, with nominal loads around 400 mA/cm^2, with a few companies presenting values as low as 200 mA/cm^2. A low current density profile will naturally limit the ability to variate the power input when coupling alkaline electrolyzers with intermittent wind energy. The only way to circumvent this will be by increasing the installed capacity, consequently increasing the investments costs.

Polymer Electrolyte Membrane Water Electrolysis

Around the 1960s, the development of an acidic solid polymer electrolyte by DuPont allowed the introduction of another concept of water electrolyzers. Polymer electrolyte membranes (PEMs) based on perfluorosulfonic acids that enabled general electric to realize PEM water electrolysis for the first time, a novel concept where a very thin solid membrane was coated with iridium and platinum powders forming the anode and cathode electrodes, respectively [13]. In the 1970s, other developments were demonstrated in a laboratory scale, where a single electrode surface of approximately 2300 cm^2 over a perfluorosulfonic acid (PFSA) membrane was fabricated. GE showed current

1. www.fch.europa.eu.

TABLE 4.2 Overview of Leading Manufacturers of Alkaline Electrolyzers

Manufacturers	Series/Operating Pressure	H_2 Rate (Nm^3/h)	Energy Consumption (kWh/Nm^3 H_2)	Partial Load Range (%)	Electrolyte/ Temperature	H_2 Purity (%)	Comment
Hydrogenics[a]	HYSTAT/10–25 bar	10–60 Maximum 15 per stack	4.9–5.4 (AC, system—all included)	40–100 (25–100 optional)	30% wt. KOH in H_2O	99.9; H_2O saturated, $O_2 < 1.000$ ppm (before HPS)	
Hydrotechnik GmbH[b]	EV Series atmospheric	40–220	5.28	20–100	30% wt. KOH in H_2O at 80°C	99.9	Cell parts are all Ni coated—200 mA/cm^2 at 2.2 V
McPhy[c]	McLyzer	10–400	4.43–5.25 (DC at nominal flow rate)	–	–	–	
NEL[d]	A-Range	50–485	3.8–4.4 (DC)	15–100	25% wt. KOH in H_2O at 80°C	99.9 before HPS	
Nuberg PERIC[e]	ZDQ Series	5–600	4.6		30% wt. KOH in H_2O at 95°C	99.8	

Sagim S.A.[f]	M Series/7 bar monopolar	1.5–5	5	0–100	65°C	99.9	Lifetime 30,000 h
Teledyne Energy Systems[g]	Titan EL-N/up to 9 bar	100–500	–	–	Water fed with min 1 M Ω-cm	9.999	
Tianjin Mainland Hydrogen Equipment[h]	FDQ Series/up to 50 bar	2–1000	4.4–4.8 (DC)	40–100	30% wt. KOH in H_2O at 90°C	99.9	Asbestos/ nonsbestos

[a] *www.hydrogenics.com*.
[b] *http://www.en.ht-hydrotechnik.de*.
[c] *www.mcphy.com*.
[d] *www.nelhydrogen.com*.
[e] *www.nubergindia.com/nuberg-hydrogen-brochure.pdf*.
[f] *http://www.sagim-gip.com*.
[g] *http://www.teledynees.com*.
[h] *http://www.cnthe.com*.

densities close to 1.8 A/cm^2 at a cell voltage of 2 V with an operating temperature of 80°C and using Nafion membranes from Dupont that were 250 μm thick. Over the following years, many other companies and research institutes dedicated themselves to further develop PEM-based electrolyzers, including but not limited to ABB in Switzerland (around 1970 and 1980) where two 100-kW systems were installed and tested. These systems were run by Stellram SA in Nyon (Switzerland) from 1987 to 1990 and by Solar-Wasserstoff-Bayern GmbH (SWB) in Neuenburg vorm Wald (Germany) from 1990 to 1996. The MEMBREL systems consisted of four modules with about 30 cells each and with an active surface area of 400 cm^2 each arranged in two vertical stacks. In Japan, Fuji Electric Corporate also worked to develop a PEM electrolyzer with a single-electrode surface of 2500 cm^2 as part of the World Energy Network (WE-NET) project from 1993 to 1998 funded by the Japanese Ministry of Economy, Trade and Industry (METI). With a five-cell short stack, cell voltages of 1.57 V were achieved at 80°C and a current density of 1 A/cm^2 under atmospheric conditions. The objective of the WE-NET project was to develop PEM electrolyzers with a single cell area of 10,000 cm^2, current densities of 1−3 A/cm^2, and an efficiency of >90% relative to the HHV of hydrogen. GenHyPEM was an STREP program supported by the European Commission in the course of the sixth framework research program. GenHyPEM gathered partners from Belgium, Germany, Romania, Federation of Russia, and France. The main goal of the project was to develop low-cost and high-pressure (50 bars) PEM water electrolyzers for the production of up to 1 Nm^{3}H$_2$/h. Over the next decades after the first GE demonstrations and work from many other groups around the world, the use of PEM water electrolyzers is still limited to small niches, such as military and space program applications, and other onsite gas generation where the electricity cost is not an issue. As discussed above, "cheap and dirty" hydrogen coming from natural gas reforming is even to this date a strong competitor to supply hydrogen to the industry. The only thing that has essentially remained is the know-how that came from these R&D activities since 1960 on PEM water electrolyzers and a handful of companies still working in this field (Fig. 4.4).

Lessons Learned From the Past

There has been an overwhelming number of scientific publications, projects, conference presentations, and much more on low-temperature fuel cells (both PEM and alkaline) since its inception. The overwhelming attention has been driven by the need of an alternative energy source, for both stationary and transport applications, a way to avoid the still dependence on pollutant fossil−based fuels. Nevertheless, over the decades we have set aside the fact that all these fuel cell hydrogen−based technologies are dependent on the same hydrogen, a fuel that presently needs to be produced from a fossil-free-based

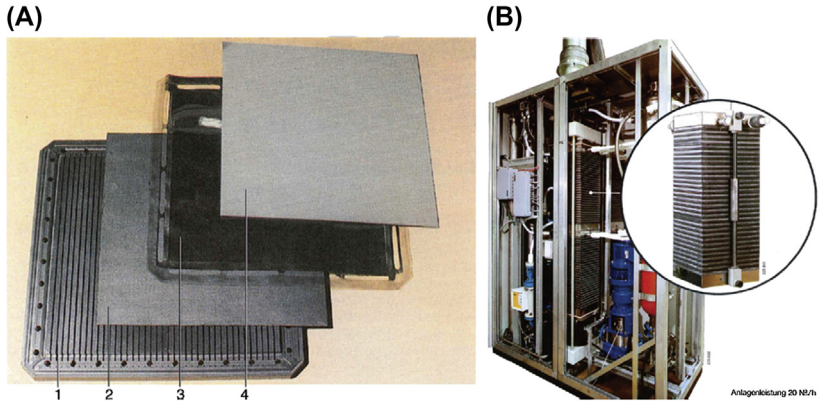

FIGURE 4.4 Components of a 400-cm^2 MEMBREL cell module (A): 1, bipolar plate made of graphite/plastic; 2, cathode current collectors made of graphite/plastic; 3, membrane; and 4, anode current collector made of sintered titanium; (B) 100-kW MEMBREL pilot plant for 20 $Nm^3\ h^{-1}$ at an operating pressure of 1−2 bar.

energy source. There has been always the hope that our so dreamed "hydrogen economy" would be still fulfilled, where even the production of hydrogen using nuclear-based energy was considered. This has led to a "knowledge" gap, where unfortunately not enough resources (both industry and governmental) have been allocated to the R&D of water electrolyzers, reflected by the marginal number of projects and consequently lack of publications and know-how dedicated to the study of both alkaline and PEM electrolyzers. Today, the prospects have finally changed, fueled by the recent "Energiewende" concept in Germany, where gigawatt seasonal and intermittent renewable electricity (wind and solar) will need to be somehow stored and where water electrolyzers will fatally play a key role in our future energy scheme. What happens now is that in the next few decades (until 2050), the technology needs to be sustainably available both in terms of efficiency and durability, and most importantly at feasible capital or installation costs. This gives us (researchers and industry) only a few more years to potentially turn both "ancient" technologies into "game changer" technologies. There is not much time left, and clear breakthroughs are necessary to, for instance, quickly increase the efficiencies to values above 70% (perhaps 80%), guarantee long-term durability of above 100,000 h, and reduce capital costs to values under 500 €/kW. Because of a said lack of consistent R&D in the past, the only thing we know is that both technologies are still based on rudimentary cell and stack designs, high load of noble metals, costly titanium-based components, and moderate to sometimes miserable performance profiles.

These conditions surely not enough to couple to renewable energy sources such as wind and PVs and be able in the future to generate a reasonable business case for large-scale (gigawatt range) water electrolyzers.

Key Players in 2018 (Research and Industry)

The constant increase in the share of renewable but intermittent energy sources will fatally change the energy matrix, where water electrolysis starts to play a key role, storing gigawatts of energy in the form of hydrogen. This is already a shortcoming reality in countries such as Germany and Denmark where a few large-scale demonstration projects already exist. For these reasons, many small, median, and fairly large enterprises are emerging in the field of water electrolyzers to be ready for a hydrogen market to come. Some of them have kept their original names, some have changed, possibly as a marketing strategy, and a few have merged or were absorbed by other companies. Table 4.3 presents a list (in alphabetic order) of the key players involved in the research, development, and/or commercialization in the field of water electrolyzers. This is not an exhaustive list, and the main objective is to present a quick overview about the main players. For obvious reasons, specific and detailed information about the companies will have to be accessed by directly contacting their specific offices, and only public information freely provided in their websites (2018) shall be presented.

TABLE 4.3 List of Key Players Involved in the Research, Development, Fabrication, and/or Commercialization in the Field of Water Electrolyzers

Companies	Businesses and Products
3M, USA	Membrane electrode assemblies (MEAs)
AGFA, Belgium	Diaphragms for alkaline electrolyzers
Areva H2Gen, France	PEM electrolyzers
Asahi Kasei, Japan	Chlor-alkali electrolysis, components
Baltic Fuel Cells, Germany	Testing hardware
Bekaert, Germany	Components
Borit NV	Bipolar plates
Chemours, France	Membranes
Covestro Deutschland AG, Germany	Chlor-alkali Electrolyzers
De Nora, Italy	Components for water electrolyzers
Dioxide Materials, USA	MEAs
Freudenberg Performance Materials SE & Co. KG, Germany	Components for water electrolyzers
FuelCon AG, Magdeburg-Barleben, Germany	Testing hardware and test stations (alkaline and PEM)

TABLE 4.3 List of Key Players Involved in the Research, Development, Fabrication, and/or Commercialization in the Field of Water Electrolyzers—cont'd

Companies	Businesses and Products
FUMATECH BWT GmbH, Germany	Components for water electrolyzers
Giner ELX Inc. Newton, MA, USA	Electrolyzer stacks and systems
GKN, UK	Components
Greenerity® GmbH, Germany	MEAs
GreenHydrogen.dk ApS, Kolding, Denmark	Electrolyzers
Greenlight Innovation, Burnaby, BC, Canada	Testing hardware and test stations (alkaline and PEM)
Haldor Topsoe, Denmark	High-temperature electrolysis
Heraeus Deutschland GmbH & Co. KG, Germany	Catalysts and components
H-TEC SYSTEMS GmbH, Lübeck, Germany	PEM electrolysis stacks and systems
Hydrogenics, Belgium	Alkaline and PEM electrolyzers
HydrogenPro, Porsgrunn, Norway	High-pressure alkaline electrolyzer plants
HyPlat (Pty) Ltd, Cape Town, South Africa	MEAs, platinum-based catalyst
HIAT GmbH, Schwerin, Germany	MEAs, platinum-based catalyst
iGas energy GmbH, Stolberg, Germany	Electrolyzer plants for hydrogen production
ITM Power Plc, Sheffield, United Kingdom	PEM electrolyzers
Johnson Matthey, United Kingdom	Precious metals and catalysts
Kumatec GmbH, Germany	High-pressure alkaline electrolyzers
McPhy Energy SA, Italy	Alkaline electrolyzers
Mott, USA	Porous transport layers and components
Nel Hydrogen, Notodden, Norway	Alkaline electrolyzers
Oerlikon Metco Coatings GmbH, Germany	Coatings
Pajarito Powder, LLC, Albuquerque, NM, USA	Catalysts
Precors GmbH, Germany	Bipolar plates
Proton OnSite, USA	PEM electrolyzers

Continued

TABLE 4.3 List of Key Players Involved in the Research, Development, Fabrication, and/or Commercialization in the Field of Water Electrolyzers—cont'd

Companies	Businesses and Products
Siemens, Germany	PEM electrolyzers
Sunfire GmbH, Germany	High-temperature electrolyzers
Thyssenkrupp Uhde Chlorine Engineers GmbH, Germany	Chlor-alkali electrolyzers
Tianjin Mainland Hydrogen Equipment, Tianjin, P.R. China	–
Toray, Japan	Components for electrolyzers
TreadStone Technologies	MEAs and bipolar plates

Principles of Water Electrolysis

The decomposition of water using free electrons consists of two electrochemical partial reactions separated by an ion-conducting electrolyte. The three typical processes used to split the water into hydrogen and oxygen are distinguished by the choice of electrolyte, with the electrolyte defining all other components inside the cell, stack, and balance of plant. In addition, the electrolyte choice shall also define the operating conditions. All these three technologies are shown in Fig. 4.5, with their respective partial reactions for the hydrogen evolution reaction (HER) and the oxygen evolution reaction.

Both alkaline and acidic (PEM) electrolyzers require liquid water to solvate the ions passing through the diaphragm (alkaline) or membrane (PEM). The water boiling temperature point will for both cases limit its operating temperature because water in the liquid form is required for transport of ions. For the solid oxide cell, O^{2-} is transported across a dense ionic conductor consisting of ZrO_2 doped with Y_2O_3 that only occurs between 700 and 1000°C, limiting again its operating temperature. For the alkaline type, usually 25%–35% wt. KOH in water is used as an electrolyte, running usually at 80–90°C, from atmospheric to pressures as high as 200 bar. Only materials that can sustain the harsh caustic conditions are selected, usually Ni- or steel-based electrodes; asbestos-, NiO-, or ZrO_2-based diaphragms; and potassium hydroxide–resistant polymer materials as frames and/or gaskets. For the PEM type, the acidic condition provided by the perfluorosulfonic acid membrane and ionomer and the high potential at the anode side (oxygen evolution) will require the use of precious metals based on iridium and platinum and the use of titanium-based components.

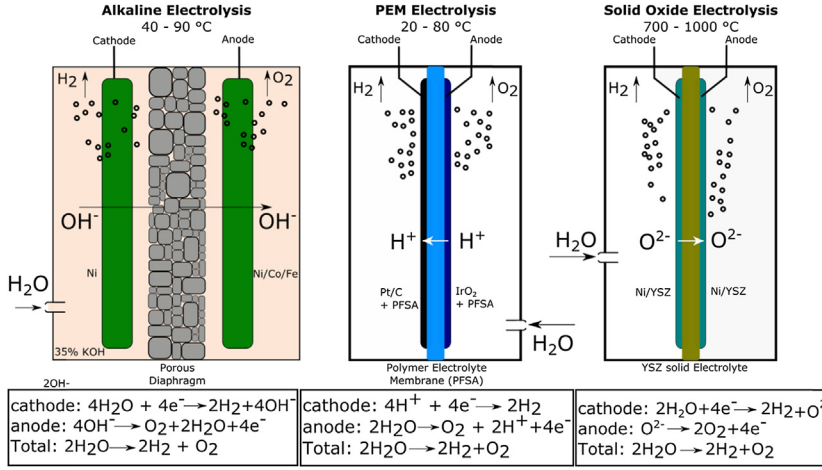

FIGURE 4.5 Operating principles of the different types of water electrolysis.

Thermodynamics

H_2O is a very thermodynamically stable molecule in our nature, a fluid responsible for the maintenance of life of most living organisms in our planet. It covers roughly 70% of the earth's surface, and around the same percentage is found inside our body. However, it contains a "valuable fuel," hydrogen. One way to harvest the H_2 molecule is by overcoming the equilibrium cell voltage, E^0, or the electromotive force by means of using free electrons, therefore electrolysis.

If two electrodes are immersed in a water-based electrolyte, and with the absence of current flow, the equilibrium potential is established, cell voltage is defined by the potential difference between anode and cathode, which turns into

$$E^0 = E^0_{\text{anode}} - E^0_{\text{cathode}} \tag{4.1}$$

In addition, Eq. (4.2) relates the change in the standard Gibbs free energy (ΔG^0) of the electrochemical reaction to the equilibrium cell voltage as follows:

$$\Delta G^0 = -nFE^0 \tag{4.2}$$

where n is the number of moles of electrons transferred in the reaction and F is the Faraday constant (96,485C).

One can calculate at a fixed temperature the $\Delta_r G^0$ for any specific reaction from

$$\Delta_r G^0 = \Delta_r H^0 - T \cdot \Delta_r S^0 \tag{4.3}$$

where ΔH^0 is the standard variation of enthalpy, T the temperature, and ΔS^0 the variation of entropy. Now using Table 4.4 with the ΔH^0 of formation and

TABLE 4.4 Thermodynamic Values Related to the Reaction $H_2O \rightarrow H_2 + {}^1/_2\, O_2$

	ΔH^0_f (kJ/mol)	ΔG^0_f (kJ/mol)	S^0 (J/mol K)
H_2O liquid	−285.83	−237.129	69.91
H_2O vapor	−241.818	−228.572	188.825
H_2 gas	0	0	130.684
O_2 gas	0	0	205.138

S^0 for the reactants and products in the water (liquid) splitting reaction, one can calculate the final $\Delta_r G^0$ at 25°C (298K) using

$$\Delta_r G^0 = \sum_{R,P}\left(\upsilon_P \Delta_f H^0_P - \upsilon_R \Delta_f H^0_R\right) - T\cdot\sum_{R,P}\left(\upsilon_P S^0_P - \upsilon_R S^0_R\right) \qquad (4.4)$$

and by filling the terms giving

$$\begin{aligned}\Delta_r G^0 =& (0\ \text{kJ/mol} + 1/2\cdot 0\ \text{kJ/mol} - (-285.83\ \text{kJ/mol})) - 298.\\ & (+0.130684\ \text{kJ/mol} + 1/2\cdot 0.205138\ \text{kJ/mol} - 0.06991\ \text{kJ/mol})\\ =& \Delta_r G^0 = +237.153\ \text{kJ/mol}(\text{for}\ H_2O \rightarrow H_2 + 1/2O_2)\end{aligned}$$

Finally, using Eq. (4.2), one can calculate the theoretical electromotive force (emf) for splitting liquid water at 25°C, giving

$$\begin{aligned}E^0 &= -\Delta G^0/nF = -237153\ \text{J/mol}/2\cdot 96485\\ &= -1.223\ \text{V}(H_2O \rightarrow H_2 + 1/2O_2)\end{aligned}$$

We can easily approximate overall water electrolysis cell potential to $E^0(25°C) = 1.23$ V and the change in Gibbs free energy as +237.2 kJ/mol, which is the minimum amount of electrical energy required to produce hydrogen and oxygen.

From the calculations above, we can start playing with different thermodynamic conditions to obtain the maximum efficiency to convert the electrical work into chemical energy (electrolysis process) and vice versa. The first thing we must notice is that the water splitting reaction is thermodynamically unfavorable and can only occur when sufficient electrical energy is supplied to overcome the reversible cell potential of 1.23 V, only for the electrochemical reaction to start. Second, the total reaction enthalpy must be supplied in the form of electrical energy, and therefore a thermoneutral voltage (1.48 V) has to be respected if one wants to avoid the generation of heat. Above 1.48 V, the reaction will be exothermic, which can be in some cases beneficial if extra heat can be supplied from another source to compensate the TΔS term that kicks in

TABLE 4.5 Different Thermodynamic Operating Conditions for the Water Splitting Reaction

	ΔH^0 (kJ/mol)	E^0 (V)	ΔG^0 (kJ/mol)	E^0 (V)
Higher heating value using liquid water	285.83	−1.48	237.15	−1.23
	Pure electric energy supply Base case for the electrolysis process		$T\Delta S$: heat supply H_2O_{vapor}: electric $H_2O_{splitting}$: electric Use of waste and/or ambient heat	
Lower heating value using liquid water	241.81	−1.25	228.57	−1.19
	$T\Delta S$: electric H_2O_{vapor}: heat supply (vapor) $H_2O_{splitting}$: electric		$T\Delta S$: heat supply H_2O_{vapor}: heat supply (vapor) $H_2O_{splitting}$: electric High-temperature electrolysis	

(use of waste or ambient heat). The same happens if, for example, water vapor can be supplied, giving another gain in terms of efficiency, definitely not negligible, in case electricity cost is a concern.

Table 4.5 summarizes this discussion, giving an overview of different possible thermodynamic conditions to operate the water electrolyzers.

In addition to Table 4.5, Fig. 4.6 shows the reversible cell potential dependence on the temperature typically found in the literature.

One can clearly notice that if only the reaction enthalpy is considered to calculate the cell voltage, a temperature increase will have a marginal effect on the final cell voltage and a significant variation is only obtained with regard to the equilibrium voltage. Nevertheless, even when the equilibrium potential is met, beyond this point the electrode reactions are inherently slow and over potentials (η_n) above the equilibrium cell voltage is needed to perform the reaction ($\eta = E_{cell} - E_0$). The overall cell overpotential (what comes above, for example, 1.23 V) can be understood as a sum of the high activation energy barrier to split the atoms (cathode + anode), ohmic resistances (electric and ionic), and mass transport limitations inside the cell/stack, giving

$$\eta_{Total} = \eta_{Anode} + \eta_{Cathode} + \eta_{Ohmic} + \eta_{Mass} \tag{4.5}$$

where

- η_{Total} is the total cell overpotential;
- η_{Anode} is the overpotential related to the activation losses at the anode;
- $\eta_{Cathode}$ is the overpotential related to the activation losses at the cathode;

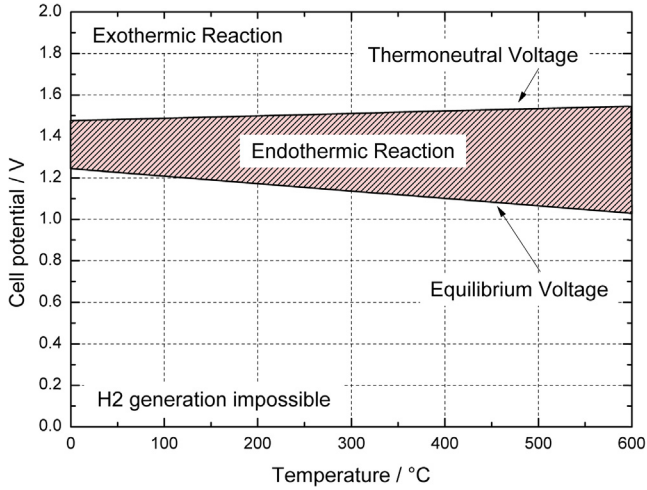

FIGURE 4.6 Cell potential at the equilibrium versus temperature for the water electrolysis reaction.

- η_{Ohmic} is the overpotential related to the sum of electric and ohmic resistances; and
- η_{Mass} is the overpotential related to losses due to mass transport limitations.

Activation Overpotential

In simple terms, the activation overpotential corresponds to the energetic barrier to be overcome to begin any oxy−redox electrochemical reaction, specifically related to the electron transfer that happens at the electrode interface. Fig. 4.7 shows a typical scheme to demonstrate this phenomenon and the key role of an electrocatalyst to lower the energy barrier for any reaction of interest.

If one considers a simple reaction where only the transference of one electron takes place in the oxy−redox reaction, we have

$$\mathrm{A} + z\mathrm{e}^- \underset{\mathrm{k_{anode}}}{\overset{\mathrm{k_{cathode}}}{\leftrightarrow}} \mathrm{B}$$

where z is the number of electrons; in this case 1, A is the oxidized specie, B is the reduced specie, $\mathrm{k_{cathode}}$ is the rate constant for the cathodic reaction, and $\mathrm{k_{anode}}$ is the rate constant for the anodic reaction.

The goal now is to determine the reaction rates for both anode and cathode, and this only considers a reaction of the first order, giving for both cathode and anode

$$\mathrm{v_{cathode}} = \mathrm{k_{cathode}}[\mathrm{A}]_{\mathrm{interface}} \tag{4.6}$$

$$\mathrm{v_{anode}} = \mathrm{k_{anode}}[\mathrm{B}]_{\mathrm{interface}} \tag{4.7}$$

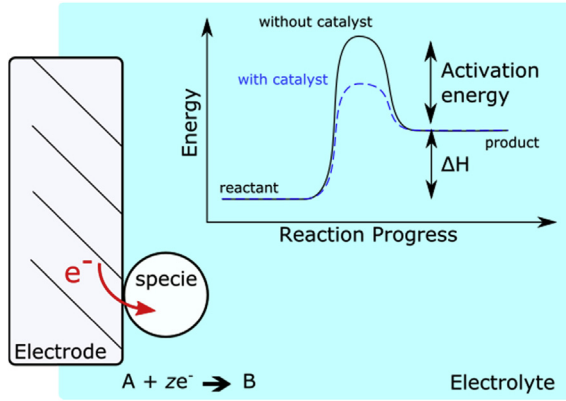

FIGURE 4.7 Activation overpotential in electrochemical reactions. An activation energy barrier has to be overcome for the reaction to take place.

By using Arrhenius, and introducing now the activation energy terms for each reaction, we can obtain each equation for the reaction rate, remaining

$$v_{cathode} = k_1^{cathode}[A]e^{-\left(\Delta G^{\#}_{cathode}/RT\right)} \tag{4.8}$$

$$v_{anode} = k_1^{anode}[B]e^{-\left(\Delta G^{\#}_{anode}/RT\right)} \tag{4.9}$$

If we now use the Faraday law ($i = F \cdot v$) for the one electron transfer reaction above, we can obtain the necessary current dependence:

$$i_{cathode} = F \cdot v_{cathode} \tag{4.10}$$

$$i_{anode} = F \cdot v_{anode} \tag{4.11}$$

The next step is to introduce the Gibbs free energy so that the activation energies for the cathode and anode in Eqs. (4.8) and (4.9) can be deconvoluted toward voltage dependence, where we use

$$\Delta G^{\#}_{cathode} = \Delta G^{\#}_{cathode*} + F\beta(E_0 + \eta) \tag{4.12}$$

$$\Delta G^{\#}_{anode} = \Delta G^{\#}_{anode*} - F(1-\beta)(E_0 + \eta) \tag{4.13}$$

Finally, by combining Eqs. (4.8), (4.10), and (4.12) for the cathode and Eqs. (4.9), (4.11), and (4.13) for the anode and assuming equilibrium state where $\eta = 0$, $i = 0$, and $i_{anode} = i_{cathode} = i_0$, we merge into the famous Butler–Volmer equation:

$$i = i_0\left\{e^{-(\beta F\eta/RT)} - e^{((1-\beta)F\eta/RT)}\right\} \tag{4.14}$$

Ohmic Overpotential

The ohmic overpotential is essentially, as its name suggests, given by the pure Ohm's law, where

$$\eta_{\text{ohmic}} = \text{RI} \tag{4.15}$$

where R is the resistance (electronic and/or ionic) and I is the current. At higher current densities, the primary electron transfer rate (activation overpotential) is no longer limiting. Hence, overpotentials will arise through slow transport of reactants from the electrolyte to the electrode surface and also obviously the transport from the surface, away from the electrode to the electrolyte. In addition, limitations or losses arising from electron resistances to/from cell or stack components can be also responsible for an increase in the ohmic overpotential.

Mass Transport Overpotential

As implied by its definition, mass transport limitation is driven by the inertia to transport species (reactants and/or products) to the electrode surface (reactants) and/or out of the electrode surface. In other words, at high current density, the electron transfer and ohmic transport will not be rate-determinant and the ability to provide new species will be the rate-determining step.

The mass transference step can be governed by three different mechanisms: (1) diffusion overpotential; (2) convection overpotential (natural and/or imposed); and (3) migration overpotential (governed by an electric field gradient).

The Nernst Equation

The standard cell potentials, which were discussed above, refer to cells in which all dissolved substances are at unit activity, which essentially means an "effective concentration" of 1 mol/L. The same approximation was used for gases that take part in the electrochemical reaction, where an effective pressure (known as the fugacity) of 1 atm is usually considered. Naturally, if different values of concentration and/or pressures are taken, the cell potential for a given electrochemical reaction will be affected, which either brings the free energy change $\Delta_r G$ toward more negative values than $\Delta_r G^0$ or more positive values than $\Delta_r G^0$. This change in the relation of $\Delta_r G$ to $\Delta_r G^0$ will consequently affect the relation from cell voltage E to the standard cell potential E^0 as well. Now, with this in mind we can combine $\Delta G = -\text{nFE}$ and $\Delta G = -\text{nF}E^0$ (Eq. 4.2) with

$$\Delta G = \Delta G^0 + \text{RTln}Q \tag{4.16}$$

and obtain

$$-\text{nFE} = -\text{nF}E^0 + \text{RTln}Q \tag{4.17}$$

which can be rearranged into

$$E = E^0 - \frac{\text{RT}}{\text{nF}}\ln(Q) \tag{4.18}$$

This is the very celebrated Nernst equation, which importantly relates the cell potential to the standard potential and to the activities of the electroactive species. As discussed above, we must notice that the cell potential will be the same as E^0 only if Q is unity. The Nernst equation is more commonly written in base 10 log forms and at 25°C we obtain

$$E = E^0 - \frac{0.059}{n}\log Q \tag{4.19}$$

This relation has a very crucial significance, where a cell potential will change by 59 mV per 10-fold change in the concentration of a substance involved in a one-electron oxidation or reduction; for two electron processes, the variation will be 28 mV per decade concentration change.

Cell Potentials Versus pH—Water Stability Diagram

Because we are strictly dealing with water oxidation here (electrolysis), naturally the electron transfer reactions will involve the transference of hydrogen ions (PEM) and hydroxide ions (alkaline). The standard potentials for these reactions therefore refer to the pH, either 0 or 14, at which the appropriate ion has unit activity. Because multiple numbers of H^+ or OH^- ions are often involved, the potentials given by the Nernst equation can vary greatly with the pH. It is frequently useful to look at the situation in another way by considering what combinations of potential and pH allow the stable existence of particular species. This information is most usefully expressed by means of an E versus pH diagram, also known as a Pourbaix diagram.

The reduction reaction using an acidic electrolyte can be written as

$$2H^+ + 2e^- \rightarrow H_2(g)$$

or in neutral or alkaline solutions as

$$H_2O + 2e^- \rightarrow H_2(g) + 2OH^-$$

These two reactions are equivalent and follow the same Nernst equation:

$$E_{\frac{H^+}{H_2}} = E^0_{\frac{H^+}{H_2}} + \frac{RT}{nF}\ln\frac{[H^+]^2}{p_{H_2}} \tag{4.20}$$

which at 25°C and H_2 with unit partial pressure gives

$$E = E^0 - 0.059\ \text{pH} = -0.059\ \text{pH} \tag{4.21}$$

Analogously, we will have for the oxidation of water

$$H_2O \rightarrow O_2(g) + 4H^+ + 2e^-$$

the following:

$$E_{\frac{O_2}{H_2O}} = E^0_{\frac{O_2}{H_2O}} + \frac{RT}{nF}\ln p_{O_2}\cdot[H^+]^4 \tag{4.22}$$

From this information we can construct the stability diagram for water that is shown in Fig. 4.8.

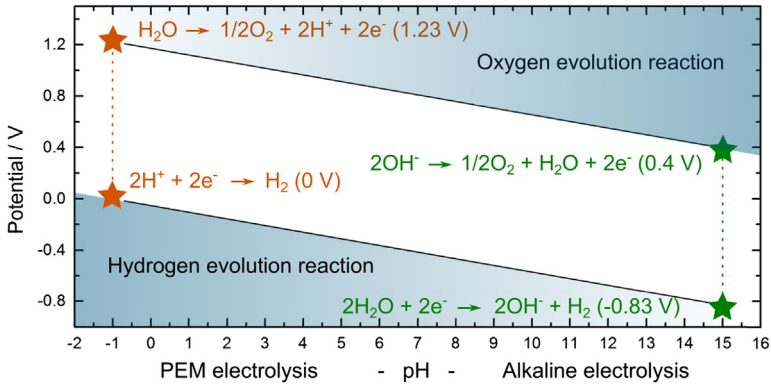

FIGURE 4.8 Stability (Pourbaix) diagram for water.

Faraday's Laws of Electrolysis

The known Faraday constant 96,485 C/mol denoted by the symbol F, or also called 1 F, corresponds to the amount of electricity that is carried by 1 mol of electrons. The number comes from the charge of a single electron 1.6023×10^{-19} C times the number of electrons in 1 mol, given by the Avogadro number 6.02×10^{23} electrons.

According to the Faraday's first law, in a given electrochemical reaction the mass (m) of substance that is deposited or released at the electrode surface is directly proportional to the amount of electricity or charge (Q) that passes through it.

$$m \; \alpha \; Q \text{ or } m = Z \cdot Q \tag{4.23}$$

where m is the mass in grams, Q is the charge in Coulombs, and Z is the proportionality number given in g/C. The proportionality number can be translated as the electrochemical equivalent (E), which is the mass produced or consumed at the electrodes by 1 C of charge. This means that 1 C will liberate 1 g equivalent of a substance divided by 96,485, where Z can be finally expressed as Z = E/96,485. Now, if we rearrange Eq. (4.23) using $Q = I \cdot t$, we obtain

$$m = \frac{E \cdot I \cdot t}{F} = \frac{M \cdot I \cdot t}{F \cdot z} \tag{4.24}$$

where m is the mass of the substance liberated at the electrode (in grams), M is the molar mass of the substance (in g/mol), I is the current (in amperes), t is the time (in seconds), F is the Faraday constant or 96,485 C, and z is the valence number of ions of the substance or the number of electrons transferred per ion.

Basic Principles of Alkaline Water Electrolysis

An alkaline electrolyzer is characterized by having two electrodes (cathode and anode) immersed in a liquid alkaline electrolyte consisting of a caustic potash solution at a level of 20%−35% KOH. Today, microporous diaphragms are almost exclusively used as separators/diaphragms in alkaline electrolysis (Fig. 4.5) with the function of keeping the product gases apart from one another for the sake of efficiency and safety. The diaphragm must also be permeable to the hydroxide ions and water molecules. Three major challenges are normally associated with alkaline electrolyzers, low partial load range, limited current density, and low operating pressure. First, the diaphragm does not completely prevent the product gases from permeating through it, leading to safety-related shutdowns at approximately 2 vol.% H_2 in O_2. The diffusion of oxygen into the cathode chamber reduces the efficiency of the electrolyzer because oxygen will be catalyzed back to water with the hydrogen present on the cathode side. Additionally, extensive mixing (particularly hydrogen diffusion to the oxygen evolution chamber) also occurs and must be avoided to preserve the efficiency and ensure a safe operation. This is particularly severe at lower current densities (<100 mA/cm^2) where the oxygen production rate decreases, thus drastically increasing the hydrogen concentration to unwanted and dangerous levels. The second drawback for alkaline electrolyzers is the low maximum achievable current density because of the high ohmic losses across the liquid electrolyte and diaphragm. Because the ZrO_2 particles and polymer mesh that gives mechanical stiffness to the diaphragm are not OH^- conductive, it contributes to an additional loss (ohmic), dramatically reducing the cell voltage efficiency at a given current. The high porosity will also lead to another challenge, the inability to operate at high pressure, which makes for a bulky stack design configuration. To operate at higher pressures, the electrodes are designed so that a given distance is obtained between them, which is a distance or spacing that will minimize the extensive mixing of gases produced at each electrode. In addition to this, electrodes that are apart from the diaphragm will eventually lead to a "curtain" of gas bubble between electrode and diaphragm, also contributing to an increase in the ohmic overpotential (the so-called "bubble resistance").

Fig. 4.8 shows an illustration with typical overpotentials for the anode and cathode of an alkaline electrolysis cell, where the most widely used electrode material is nickel because of its stability and favorable activity in high concentrated KOH solutions. One can notice that, in contrast to PEM electrolysis (acidic media), the cell voltages are more or less distributed between cathode and anode. In general words, however, the overpotential of oxygen evolution is more challenging for real cells than that related to the HER (cathode). Moreover, the oxidizing regime will fatally reduce any catalyst material to its oxidized form, severely reducing the surface area

because of a passivation phenomenon on the catalyst surface. On the cathode side, hydride phase formation that leads to electrode deactivation seems to be a concern, especially if pure Ni electrodes are used.

Basic Principles of Polymer Electrolyte Membrane Water Electrolysis

The concept idealized by Grubb at GE, where a solid perfluorosulfonic membrane is used as an electrolyte, also referred to as proton exchange membrane or polymer electrolyte membrane (PEM) water electrolysis, is responsible for providing high proton conductivity, relatively low gas cross-over, compact system design, and high pressure operation. The thin polymer membrane (typically 200 μm thick) is in part the reason for many of the advantages of PEM electrolyzers. In contrast to alkaline electrolysis, it can operate at much higher current densities, capable of achieving values above 10 A/cm^2, drastically reducing the investment cost of electrolyzers. The solid polymer membrane allows for a much thinner electrolyte than the alkaline electrolyzers.

The relatively low gas crossover rate of the polymer electrolyte membrane (yielding hydrogen with high purity) allows for the PEM electrolyzer to work under a wider range of power input. This is due to the fact that the proton transport across the membrane responds quickly to the power input, not delayed by inertia as in liquid electrolytes blocked by porous and high ohmic resistant diaphragms. As discussed before, in alkaline electrolyzers operating at low load, the rate of hydrogen and oxygen production reduces, while the hydrogen permeability through the diaphragm remains constant, yielding a larger concentration of hydrogen on the anode (oxygen) side, thus creating hazardous and less efficient conditions. In contrast with alkaline electrolysis, PEM electrolysis covers practically the full nominal power density range, eventually reaching values over 100% of nominal rated power density, where the nominal rated power density is derived from a fixed current density and its corresponding cell voltage. This is due to the lower permeability of hydrogen through Nafion compared with, for example, Zirfon diaphragms for alkaline electrolyzers. A solid electrolyte allows for a compact system design with strong/resistant structural properties, in which high operational pressures (equal or differential across the electrolyte) are achievable. The high pressure operation of an electrolyzer brings the advantage of delivering hydrogen at a high pressure (sometimes called electrochemical compression) for the end user, thus requiring less energy to further compress and store the hydrogen. It also diminishes the volume of the gaseous phase at the electrodes, thus significantly improving product gas removal, which follows Fick's law of diffusion. In a differential pressure configuration, only the cathode (hydrogen) side is under pressure, which can eliminate the hazards related to handling pressurized oxygen and the possibility of self-ignition of Ti in oxygen. The

pressure increase minimizes the expansion and dehydration of the membrane, preserving the integrity of the catalytic layer. Problems related to higher operational pressures in PEM electrolysis are also present, such as cross-permeation phenomenon that increases with pressure. Pressures above 100 bar will require the use of thicker membranes (although more resistant) and internal recombination catalysts to maintain the critical concentrations (mostly H_2 in O_2) under safety threshold (2 vol.% H_2 in O_2). Lower gas permeability through the membrane (crossover) can be obtained by incorporating miscellaneous fillers inside the membrane material, but this normally leads to less conducting materials. The corrosive acidic regime provided by the proton exchange membrane requires the use of distinct materials. These materials must not only resist the harsh corrosive low pH condition but also sustain the high applied voltage, especially at high current densities. Corrosion resistance applies not only for the catalysts used but also for the porous transport layers (PTLs) and bipolar plates. Only a few materials can be selected that would perform in this environment. This will demand the use of scarce, expensive materials and components such as noble catalysts (platinum group metals [PGMs], e.g., Pt, Ir, and Ru), titanium-based current collectors, and bipolar plates. Iridium has one particular limitation because it is one of the rarest elements in the earth's crust, having an average mass fraction of 0.001 ppm in crustal rock. Conversely, gold and platinum are 40 times and 10 times more abundant, respectively.

Design and Operation of Cells, Stacks, and Systems

When running electrochemical reactions in real single cells and stacks, an extensive variety of aspects and parameters when designing cell and stack hardware ought to be considered. Properly defining the operating conditions is also crucial, so that maximum efficiency, both voltage and faradaic, can be achieved, and acceptable durability is demonstrated. As discussed above, undesirable overpotentials shall arise when electrochemical systems are out of equilibrium. If one manages to accurately design cells and stacks, and intelligently choose the operating conditions, we will surely demonstrate cost-effective electrolysis devices that present low ohmic losses and mass transport limitations.

As discussed above, what essentially differentiates the two technologies is the use of caustic KOH solution for the alkaline type and the high anodic overpotential and acidic condition for the PEM. These requirements will impose the use of specific materials and components and consequently limit its design and choice of materials. As we expand the active area of electrodes and components, complexity in terms of manufacturing and assembling starts to play a crucial role. As these cells become "too large" with areas beyond 1 m^2, the costs involved will eventually turn scaling-up approaches impracticable.

Much more challenging if, for instance, high pressure operation is required. Cells and stacks have been historically manufactured using a round design, so that the pressure distribution inside the stack is adequate to provide distributed electrical contact and reactants flow, avoid the leakage of gas and fluids, prevent failures, and provide long-term durability under high pressure operation. As an advantage, there is a consequent waste of materials when cutting, a cost that increases almost linearly with scaling-up. That is the reason why multikilowatt/multimegawatt stacks are preferably rectangular. However, tradition in manufacturing alkaline stacks still maintains its round shape because dealing with liquid KOH in a rectangular shape and under pressure is not trivial.

When putting components together, either at the cell or stack level, it is crucial to obtain very low contact resistances between the components. That is the reason why PEM water electrolyzers use a catalyst-coated membrane concept, where the electrode is directly coated on the membrane, reducing the ohmic drop between them. Next is to obtain a good electrical contact between the electrode and titanium PTL and finally between the PTL and bipolar plate. When assembling the cell or stack, too less torque (or cell pressure) will lead to unacceptable low electrical conductivities across the layers and potential leakage issues. On the other hand, too much torque will transfer stress to the least mechanical resistant components such as catalyst layer, membrane, and carbon PTLs. This will cause its destruction, collapse of the necessary porosity avoiding the entrance of reactants, membrane creping, and a rapid increase in the mass transport losses inside the stack. Besides the critical loss in the cell efficiency, too much stress shall also limit the lifetime of the components because an optimal humid condition is necessary to guarantee the lifetime of electrodes and membranes. The same reasoning applies for the alkaline type, where a compromise between the mechanical integrity of the components and contact pressure has to be determined.

As an advantage for the alkaline case, liquid KOH will guarantee good OH^- transport across all components, as long as KOH can fully achieve the reaction sites. In this case, the only thing to avoid is the lack of electrical contact between electrodes and PTLs (Ni mesh), especially when using a bipolar plate configuration.

To enhance the contact between the PTL and catalyst layer, and between the PTL and bipolar plate, it is sometimes required to coat the PTL with PGM-based materials. This also to increase the lifetime of PEM stacks, by reducing the overtime passivation and dissolution of Ti-based PTLs. In addition, PGM coating should also reduce embrittlement of the materials on the cathode side. PGM coating on both PTL and bipolar plates is also a must, if cell voltages beyond 2 V are obtained, increasing the chances of irreversible degradation inside the components at the anode side of PEM electrolyzers. In an alkaline regime, one approach to reduce the cost is to substitute the use of raw Ni to fabricate the bipolar plates, by using stainless steel plates

coated with Ni. Important here is to obtain a homogeneous coating free of irregularities, which is also resistant to 30% KOH at 80–90°C.

In a bipolar plate configuration, each separator plate is responsible to separate the gases and the flow field responsible to provide an even supply of water (or reactants) over the PTL. The flow field should also release the produced gases (counterflow). Flow fields are not necessarily important when low active areas are used, as long as water is sufficiently provided to all reaction sites. However, as large electrode areas are needed for multikilowatt or multimegawatt systems, flow fields become essential so that a minimum pressure drop to circulate the reactant or cooling water is obtained. Fig. 4.9 shows the different designs or patterns that can be used in flow fields; pin-type, parallel, serpentine, parallel serpentine, eventually 3D-wire mesh, expanded metal sheets or perforated plates (Fig. 4.10).

The most common for PEM electrolysis is the serpentine type, whereas expanded mesh or perforated plates are commonly used in alkaline electrolyzers. The major drawback to the use of flow fields in separator plates is the machining cost related to its manufacturing. Machining each individual part requires large processing times and incurs rather large material waste as well as increased material thicknesses, ultimately increasing ohmic losses. A PGM coating step is also tremendously expensive and requires the use of expensive precious metals, complex equipment, and rare expertise. The use of thinner materials reducing manufacturing time can cause significant reductions in the overall stack cost. Owing to the need for flow fields to facilitate even water distribution in cells with larger active areas, a flow field must be incorporated. To include the flow field in the separator plate, the plate thickness must be at least 2–3 mm while the stamped and hydroformed components can easily

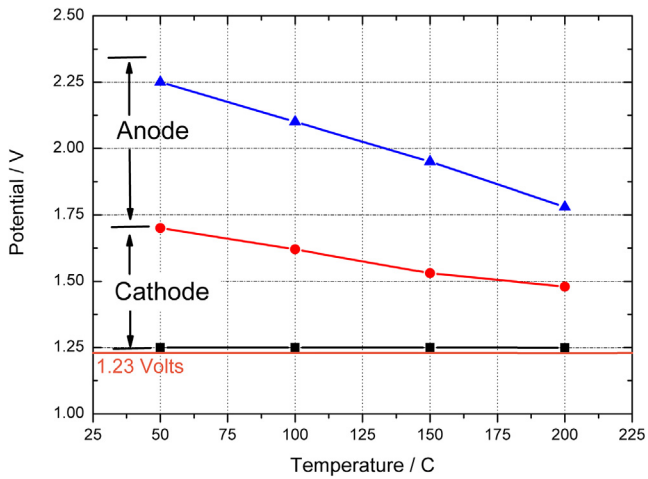

FIGURE 4.9 An illustration of the contributions of anode and cathode overpotentials of an alkaline electrolysis cell.

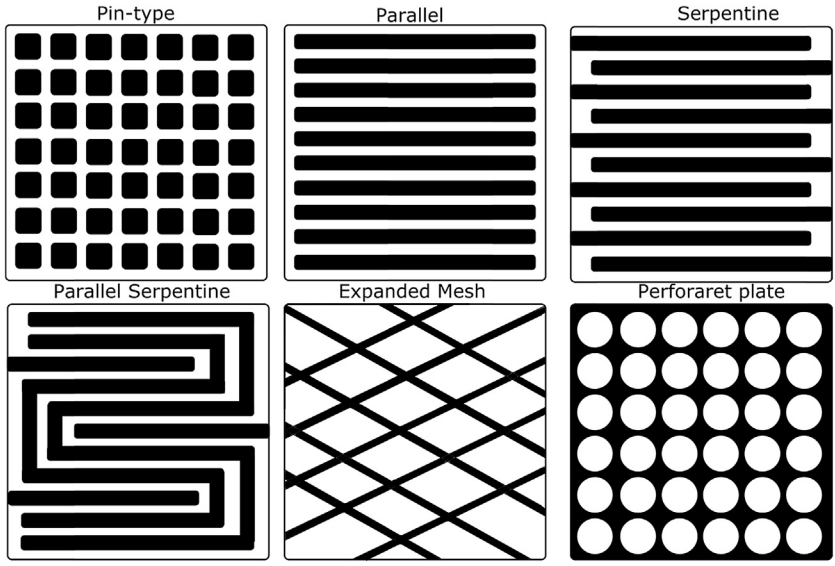

FIGURE 4.10 Typical flow-field patterns used in water electrolyzers.

reach thicknesses as small as 0.1 mm. Avoiding the incorporation of the flow field in the separator plate as the case for alkaline electrolyzers can, however, drastically reduce the manufacturing costs, thus removing the need for expensive machining or stamping processes.

ACKNOWLEDGMENTS

We would like to thank Prof. Ralf Peters and Dr. Thomas Grube, Forschungszentrum Jülich GmbH, Jülich, Germany, for the innumerous inspiring discussions and assistance in the preparation of this chapter.

REFERENCES

[1] M. Robinius, et al., Linking the power and transport Sectors-Part 2: modelling a sector coupling scenario for Germany, Energies 10 (7) (2017).

[2] M. Robinius, Strom- und Gasmarktdesign zur Versorgung des deutschen Straßenverkehrs mit Wasserstoff, RWTH Aachen University, Jülich, 2015.

[3] L. Bertuccioli, A. Chan, D. Hart, F. Lehner, B. Madden, E. Standen, Development of Water Electrolysis in the European Union - Final Report, E4tech Sàrl/element energy, Lausanne/ Cambridge, 2014.

[4] M. Reuss, et al., Seasonal storage and alternative carriers: a flexible hydrogen supply chain model, Appl. Energy 200 (2017) 290−302.

[5] T. Grube, Passenger car drive cycles, in: Fuel Cells: Data, Facts and Figures, Wiley-VCH Verlag GmbH & Co. KGaA, 2016, pp. 12−21.

[6] A. Boretti, Advances in hydrogen compression ignition internal combustion engines, Int. J. Hydrogen Energy 36 (19) (2011) 12601−12606.

[7] U. Eberle, B. Muller, R. von Helmolt, Fuel cell electric vehicles and hydrogen infrastructure: status 2012, Energy Environ. Sci. 5 (10) (2012) 8780−8798.

[8] T. Grube, Potentiale des Strommanagements zur Reduzierung des spezifischen Energiebedarfs von Pkw, Technische Universität Berlin, Jülich, 2014.

[9] Collaboration, J.-J.R.C.-E.-C., Well-to-Wheels Analysis of Future Automotive Fuels and Powertrains in the European Context - Tank-to-wheels Report, European Commission, Joint Research Centre, 2011.

[10] M. Schemme, P. Peters, R.C. Samsun, T. Grube, D. Stolten, Alternative transport fuels and their production using surplus electricity, water and CO_2, in: AIChE Annual Meeting, 2016. San Francisco.

[11] W.L. Becker, et al., Production of Fischer-Tropsch liquid fuels from high temperature solid oxide co-electrolysis units, Energy 47 (1) (2012) 99−115.

[12] N. Merdes, R. Pätzold, N. Ramsperger, H.-G. Lehmann, Die neuen R4-Ottomotoren M270 mit Turboaufladung, in: ATZ - Automobiltechnische Zeitschrift, 2012, pp. 58−63.

[13] M. Carmo, et al., A comprehensive review on PEM water electrolysis, Int. J. Hydrogen Energy 38 (12) (2013) 4901−4934.

[14] W. Hug, et al., Highly efficient advanced alkaline electrolyzer for solar operation, Int. J. Hydrogen Energy 17 (9) (1992) 699−705.

[15] A. Szyszka, Schritte zu einer (Solar-) Wasserstoff-Energiewirtschaft. 13 erfolgreiche Jahre Solar-Wasserstoff-Demonstrationsprojekt der SWB in Neunburg vorm Wald, 1999. Oberpfalz.

[16] H. Barthels, et al., Phoebus-Julich: an autonomous energy supply system comprising photovoltaics, electrolytic hydrogen, fuel cell, Int. J. Hydrogen Energy 23 (4) (1998) 295−301.